



# Kinetic modeling, optimization of biomass and astaxanthin production in *Spirogyra* sp. under nitrogen and phosphorus deficiency

Nadia Delfi Zafira<sup>1</sup>, Malvin Yulius Christian Pakpahan<sup>1</sup>, I Putu Ikrar Satyadharma<sup>1</sup>, Khairul Hadi Burhan<sup>2</sup>, Erly Marwani<sup>2\*</sup>

<sup>1</sup>Bioengineering Program, School of Life Sciences and Technology, Institut Teknologi Bandung. Kampus ITB Jatinangor 45363, West Java, Indonesia

<sup>2</sup>School of Life Sciences and Technology, Institut Teknologi Bandung. Kampus ITB Jatinangor 45363, West Java, Indonesia

\*Corresponding author: erly@sith.itb.ac.id

SUBMITTED 2 March 2023 REVISED 16 June 2023 ACCEPTED 13 September 2023

**ABSTRACT** This study studied the optimum nitrogen (N) and phosphorus (P) concentrations for biomass and astaxanthin production in *Spirogyra* sp. *Spirogyra* sp. was cultivated in Blue Green (BG) medium with N/P concentrations adjusted to 1.1/0.01; 1.1/0.03; 1.1/0.06; 1.1/0.09; 2.2/0.01; 2.2/0.03; 2.2/0.06; 2.2/0.09; 4.4/0.01; 4.4/0.03; 4.4/0.06; 4.4/0.09, 6.6/0.01; 6.6/0.03; 6.6/0.06 and 6.6/0.09 mM. The results showed an increase in biomass accumulation for lower concentrations of N and N:P ratio with the highest accumulation at N/P 1.1/0.03 mM, i.e. 485 mg<sub>dryweight</sub> and a growth rate of 0.22 d<sup>-1</sup>. Astaxanthin accumulation was also found to increase, with the highest at N/P 1.1/0.01 mM, i.e. 0.269 mg/g<sub>dryweight</sub>, on the 12<sup>th</sup> day of cultivation. Based on biomass and astaxanthin accumulation, the highest astaxanthin productivity was 0.07 µg/cm<sup>2</sup>/d at N/P concentration 1.1/0.09 mM. Kinetic models were developed using the Haldane and Luedeking–Piret equations. The growth and astaxanthin production parameters obtained were  $\mu_{max}$  0.18±0.02 d<sup>-1</sup>,  $k_N$  68.2 ± 24.2 mg/L,  $k_i$  301.8 ± 78.5 mg/L,  $Y_N$  0.93 ± 0.68 g<sub>biomass/nitrate</sub>,  $\alpha$  0.36 ± 0.69,  $\beta$  -0.01 ± 0.02, and  $K_A$  0.04 ± 0.03, thus indicating that a lower N concentration is suitable for the cultivation of *Spirogyra* sp. In conclusion, *Spirogyra* sp. should be cultivated under nitrogen deficiency for continuous astaxanthin production.

**KEYWORDS** Astaxanthin; Kinetic modeling; Nutrient limitation; *Spirogyra* sp.

## 1. Introduction

Astaxanthin is a carotenoid compound that can capture reactive oxygen species (ROS) and neutralize free radicals (Lima et al. 2021). This is possible since its structure comprises a non-polar polyene chain and polar terminal rings on both ends with 13 conjugated double bonds (Ermavitalini et al. 2021). This structure also enables astaxanthin to be easily incorporated into the cell membrane (Stachowiak and Szulc 2021). Due to these characteristics, astaxanthin has a very high antioxidant property, which is 6,000 times that of vitamin C, 800 times of coenzyme Q, 500 times of  $\alpha$ -tocopherol, and 11 times of  $\beta$ -carotene (Ekpe et al. 2018; Zhuang and Zhu 2021).

In addition to being an antioxidant, astaxanthin has anti-inflammatory, anti-apoptotic, and anti-proliferative properties. It is frequently used as an anti-aging, anti-cancer, and anti-diabetic agent, as well as a protective agent for the nerve, muscle, and skin cells in cosmetic and health products (Kohandel et al. 2021; Lima et al. 2021). The market demand for astaxanthin continues to grow because of its many and varied benefits. The astaxanthin market is projected to maintain this continu-

ous growth trend with a compound annual growth rate of 17.2% (Grand Review Research 2022). As such, astaxanthin production must rise to meet the demands of local and global markets.

Astaxanthin can be synthesized by various organisms, including crabs, krill, algae, and yeast (Ambati et al. 2014). At present, the microalgae *H. pluvialis* serves as the main source of the astaxanthin used in industrial-scale production. However, its use also has certain drawbacks including slow growth, low cell density, and the high cost of cultivation and downstream processes (Tran et al. 2019; Tharek et al. 2020). Hence, a potential alternative is needed to overcome these drawbacks.

*Spirogyra* sp. is an unbranched filamentous green macroalgae that is commonly found in Indonesian freshwaters such as rice fields, ponds, rivers, and lakes (Wong-sawad and Peerapornpisal 2015). While *Spirogyra* sp. is currently a frequently used fishing bait, it is also a potential source of astaxanthin with an astaxanthin content of 0.07% (d.w.) (Pacheco et al. 2015). This value exceeds that of other astaxanthin-producing green algae such as *Chlorella zofingiensis* (0.001%), *Ulva lactuca* (0.01%), and *Catenella repens* (0.02%) (Ambati et al. 2014).

To generate stable astaxanthin production from *Spirogyra* sp., a controlled cultivation method is needed. In addition, astaxanthin production can be increased through the application of a stress-induced growth environment to *Spirogyra* sp. cultivation. A previous study showed that astaxanthin production in *Coleastrum* sp. was enhanced through the introduction of ROS as a stress inductor into the cultivation medium, which increased production by 1.3-fold (Tharek et al. 2020). Nitrogen (N) and phosphorous (P) are both essential for algal growth and therefore play an important role in astaxanthin productivity (Fan et al. 2021; Li et al. 2022). It is also known that the limited presence of N and P leads to an increase in astaxanthin accumulation in algae (Ding et al. 2019; Li et al. 2022). In addition, a low N:P ratio can increase astaxanthin production (Liu 2018). To achieve high astaxanthin productivity, research is needed to determine the optimum concentrations of N and P, along with the optimal N:P ratio for biomass and astaxanthin accumulation in *Spirogyra* sp.

In this study, the optimal concentrations of N and P, and the optimal N:P ratio for the accumulation of biomass and astaxanthin in *Spirogyra* sp. were determined from experimental results. Kinetic modeling was used to perform cultivation simulations, with the parameters obtained through parameter estimation. The parameters used for the kinetic models consist of the growth rate of *Spirogyra* sp., nitrate consumption, and astaxanthin production. Commonly used equations include the Monod, Haldane–Andrews, and Luedeking–Piret models (Abdulrasheed et al. 2020). The model that is developed can then be used as the basis for developing pilot-scale cultivation.

## 2. Materials and Methods

### 2.1. Plant material

*Spirogyra* sp. culture, which is better known by the local name lukut, was obtained from rice fields in Bojong Village, Majalaya District, Bandung Regency, West Java (LS 7°2'20" BT 107°46'28"). The collected green algae showed unbranched filaments and spirally coiled chloroplasts (Figure 1). It was confirmed as *Spirogyra* sp.

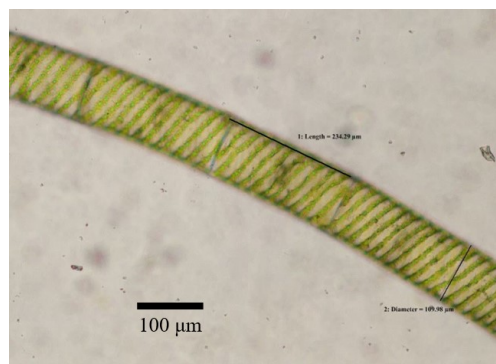


**FIGURE 1** *Spirogyra* sp. filament morphology observed under microscope with a 100x magnification.

based on its natural habitat, where it was found, and its morphological appearance. According to Takano et al. (2019), *Spirogyra* species are generally found in freshwater river streams, natural pools, or artificial freshwater pools. Moreover, morphologically, these green algae show the structure of a filament without branches, which is an elongated cylindrical cell resembling a ribbon, containing chloroplasts that are structured spirally.

### 2.2. Cultivation medium

A modified Blue Green (BG) medium was used as the cultivation medium in this study (Munir et al. 2015). The medium was modified by varying the concentrations of N and P, namely to N/P 1.1/0.01; 1.1/0.03; 1.1/0.06; 1.1/0.09; 2.2/0.01; 2.2/0.03; 2.2/0.06; 2.2/0.09; 4.4/0.01; 4.4/0.03; 4.4/0.06; 4.4/0.09, 6.6/0.01; 6.6/0.03; 6.6/0.06 and 6.6/0.09 mM. The BG medium composed of NaNO<sub>3</sub> 1.5 g/L; K<sub>2</sub>HPO<sub>4</sub> 40 mg/L; MgSO<sub>4</sub> 75 mg/L; CaCl<sub>2</sub> 36 mg/L; Citric Acid 6 mg/L; Ammonium Iron (III) Citrate 6 mg/L; Na<sub>2</sub>EDTA 10 mg/L; Na<sub>2</sub>CO<sub>3</sub> 20 mg/L; H<sub>3</sub>BO<sub>3</sub> 2.86 mg/L; MnCl<sub>2</sub> 1.81 mg/L; ZnSO<sub>4</sub> 0.22 mg/L; Na<sub>2</sub>MoO<sub>4</sub> 0.39 mg/L; CuSO<sub>4</sub> 0.08 mg/L; and Co(NO<sub>3</sub>)<sub>2</sub> 0.05 mg/L. These materials were obtained from Merck KGaA, Germany.

### 2.3. Medium preparation

BG medium was used in the cultivation of green algae *Spirogyra* sp. (Allen and Stanier 1968). Our preliminary study indicated that *Spirogyra* sp. showed the highest growth in 25% BG medium when cultivated in 2.5%; 25%; 50%; and 100% BG medium. Therefore, in this study, the availability of N and P in the medium was varied to 0.25; 0.5; 1.0; and 1.5 times the control concentration of 25% BG medium. The concentrations of N in the medium were altered to 93.75; 187.5; 375.0; and 562.5 mg/L NaNO<sub>3</sub>, while those of P varied to 2.5; 5.0; 10.0; and 20.0 mg/L K<sub>2</sub>HPO<sub>4</sub>. All the weighted components in the medium were dissolved in 4 L of distilled water to produce a 25% BG medium. The pH value of the medium was then adjusted by adding 0.1 N NaOH or 0.1 N HCl to a value of 7.5 ± 0.25 (Munir et al. 2015).

### 2.4. *Spirogyra* sp. cultivation

*Spirogyra* sp. culture was grown in 1 L of the medium in 1.5 L thin-walled containers (14 × 14 × 8 cm) with three repetitions for each treatment (Figure 2). The *Spirogyra* sp. cultivation was performed at room temperature with a light intensity of 1700–2200 lux (23–30 μmol<sub>photon</sub>/m<sup>2</sup>s) with aeration of 0.2 vvm (volume/volume/minute) (Simanjuntak 2021). A 24-hour lighting period was applied during cultivation and the *Spirogyra* sp. was cultivated for 14 days. During cultivation, the pH of the medium was checked and adjusted every 2 days to ensure it remained within the range of 7.5 ± 0.25. The pH was adjusted in line with the methods outlined by Yu et al. (2022) and the temperature was set to a constant 22 °C.

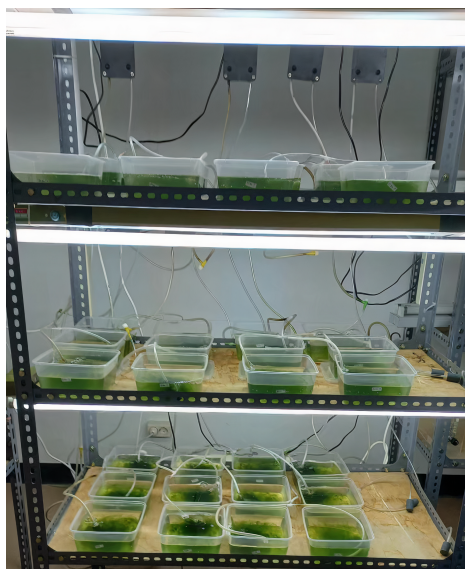


FIGURE 2 Cultivation of *Spirogyra* sp.

## 2.5. Sample harvesting

Samples were harvested every 3 d within 14 d of cultivation, on days 0, 3, 6, 9, 12, and 14. The *Spirogyra* sp. filament was drained from the cultivation container using an iron strainer. The samples were then dried in an oven (Zhao et al. 2016). The obtained biomass was further analyzed for its astaxanthin content using High-Performance Liquid Chromatography (HPLC). In addition, 1–10 mL of medium was taken for nitrate concentration analysis.

## 2.6. Measurement of dry biomass

A container (6.5 × 6.5 × 1 cm) made of parchment paper was weighed first ( $m_1$ ). The filtered sample was then placed into the container and dried in an oven following the methods of Cong et al. (2019) at 50 °C before it was weighed again ( $m_2$ ). The dry weight of the sample was determined using Equation 1.

$$\text{dry biomass (g)} = m_2 - m_1 \quad (1)$$

## 2.7. Measurement of nitrate concentration

The concentration of nitrate in the medium was measured using a spectrophotometric method (Kurniawati et al. 2017). A total of 1–10 mL of the medium was placed into a 250 mL beaker glass. The sample was dissolved using distilled water until the volume of the solution reached 50 mL with a volume of 1 mL of 1 N HCl was then added to the sample and vortexed. The mixture was first incubated for 30 min before the absorbance was measured at  $\lambda$  220 nm and 275 nm. The absorbance value was then matched with the standard nitrate curve equation to determine the nitrate concentration in the sample. Nitrate concentrations were obtained using Equation 2.

$$[\text{Nitrate}] \left( \frac{\text{mg}}{\text{L}} \right) = 20 \times (OD_{220} - OD_{275}) - 0.219 \quad (2)$$

## 2.8. Astaxanthin extraction

*Spirogyra* sp. dry biomass was ground using a mortar and pestle. Extraction was performed by maceration, following the methods of Ruen-ngam et al. (2010) with modifications. In this case, the solvent volume was 5 mL. Extraction was conducted in an incubator shaker and agitation speed of 100 rpm. The extract was then filtered using a syringe and fat-free cotton. The remaining extract in the syringe and the fat-free cotton were rinsed with 5 mL of acetone. The filtered extract was then evaporated and re-dissolved in HPLC-grade methanol for analysis using the HPLC method.

## 2.9. Astaxanthin analysis using HPLC

*Spirogyra* sp. extract was evaporated using an evaporating dish at room temperature. The dry residue of the extract was then dissolved with 5 mL of HPLC-grade methanol. Next, the sample solution was filtered using a 0.22  $\mu\text{m}$  PTFE (polytetrafluoroethylene) syringe filter into an HPLC vial. The vial was placed in the autosampler chamber of the HPLC (Shimadzu Autosampler SIL-20AC) equipped with a photodiode array (PDA) detector. The analysis was performed using a C-18 reverse phase column and HPLC grade methanol: aquabidest (95:5 v/v) as the eluent. The flow rate used was 1 mL/min and the column temperature was 25 °C. Wavelength detection was based on the methods of Régnier et al. (2015) and Karnila et al. (2021). The standard astaxanthin used was astaxanthin 97% obtained from Sigma-Aldrich, Germany. The astaxanthin content in the samples was then quantified using Equation 3 and 4.

$$[\text{Astaxanthin}] \left( \frac{\text{mg}}{\text{L}} \right) = A \times 10^{-4} - 0.0934 \quad (3)$$

$$\text{Astaxanthin} \left( \frac{\text{mg}}{\text{g}} \right) = \frac{[\text{Astaxanthin}] \times V(\text{L})}{m_{\text{sample}}(\text{g})} \quad (4)$$

Where [Astaxanthin] is the astaxanthin concentration in the sample, A is the peak area, V is the solvent volume, and  $m_{\text{sample}}$  is the mass of *Spirogyra* sp. extracted.

## 2.10. Estimation of *Spirogyra* sp. astaxanthin productivity

Astaxanthin productivity was estimated using parameters including cultivation volume (V), mass of *Spirogyra* sp. during harvesting (m), depth of cultivation area (h), astaxanthin content in the biomass of *Spirogyra* sp. (A), and cultivation time (t). The productivity of astaxanthin can be quantified using Equation 5.

$$\text{Productivity} \left( \frac{\mu\text{g}}{\text{cm}^2\text{d}} \right) = \frac{A \left( \frac{\mu\text{g}}{\text{g}} \right) \times m(\text{g}) \times h(\text{cm})}{V(\text{cm}^3) \times t(\text{d})} \quad (5)$$

## 2.11. Kinetic modeling

Kinetic modeling for *Spirogyra* sp. cultivation was performed using MATLAB® (R2018a) and SIMULINK. The

parameter estimation application on SIMULINK was used to estimate growth parameters with initial values obtained from research data. Biomass growth was modeled using the Haldane equation (6).

$$\frac{dX}{dt} = \mu X = \mu_{max} \left( \frac{N}{k_N + N + \frac{N^2}{k_i}} \right) X \quad (6)$$

Where X is biomass,  $\mu$  is the growth rate,  $\mu_{max}$  is the maximum growth rate, N is nitrate concentration,  $k_N$  is the half-saturation constant for nitrate,  $k_i$  is the half-inhibition constant for nitrate, and t is time.

For the modeling, the value of  $\mu$  is estimated using equation (7) which is obtained from the experiment data (Zhang et al. 2018).

$$\mu_{max} = Max \left[ \frac{\ln(X_{i+1} - X_i)}{t_{i+1} - t_i} \right] \quad (7)$$

Where  $X_{i+1}$  and  $X_i$  are biomass data taken during times  $t_{i+1}$  and  $t_i$

Nitrate consumption in the medium was modeled using the Haldane equation (8) and astaxanthin production was modeled using the modified Luedeking–Piret equation (Serri et al. 2020) (9).

$$\frac{dN}{dt} = -\frac{1}{Y_N} \times \mu X = -\frac{1}{Y_N} \mu_{max} \left( \frac{N}{k_N + N + \frac{N^2}{k_i}} \right) X \quad (8)$$

$$\frac{dA}{dt} = \alpha \times \mu \times X + \beta \times X - k_A \times X^2 \mu_{max} \quad (9)$$

Where N is nitrate concentration,  $Y_N$  is the biomass per nitrate yield coefficient,  $\mu$  is the growth rate, X is biomass, A is product concentration,  $\alpha$  is the growth-associated astaxanthin production coefficient,  $\beta$  is the non-growth associated astaxanthin production coefficient, and  $k_A$  is the astaxanthin consumption rate coefficient.

## 2.12. Statistics analysis

In this study, a one-way ANOVA statistical test was conducted to determine the significance of the treatment on the accumulation of biomass and astaxanthin. A post-hoc test using Duncan's method was also performed to determine the significance of the treatment between groups. In addition, the data obtained were represented as mean  $\pm$  SD (standard deviation) of a triplicate of experiments using Microsoft Excel XP. Furthermore, the correlation test between parameters was analyzed using the Pearson correlation coefficient (r) parameter. The three statistical tests were carried out using SPSS Statistics 25 software.

## 3. Results and Discussion

### 3.1. Effect of N concentration, P concentration, and N:P ratio on *Spirogyra* sp. biomass accumulation

In this study, *Spirogyra* sp. was cultivated for 14 days. The growth curve of *Spirogyra* sp. showed continuous growth

until it reached the highest biomass accumulation on day 14 (Figure 3).

The highest biomass accumulation on the 14<sup>th</sup> day was found in N/P concentration 1.1/0.01 mM with a value of  $485 \pm 31.9$  mg<sub>dryweight</sub>, while the lowest biomass accumulation was found in the N/P variation of 6.6/0.03 mM with a value of  $194 \pm 25.8$  mg<sub>dryweight</sub>. In all variations, biomass showed growth from day 0 to 12 except for variations in N/P 4.4/0.03, 6.6/0.01, and 6.6/0.03 mM. It may be caused by an initial lag period as an adaptation time for denitrification of the macroalgae due to the high concentration of nitrate present in the cultivation medium (Nalcaci et al. 2011; Serri et al. 2020). The biomass cultivation result showed that the concentrations of N and P in the medium had a significant effect on the biomass accumulation of *Spirogyra* sp. (Table 1). The result generally showed that the biomass accumulation for *Spirogyra* sp. was the greatest at a lower N concentration, namely 1.1 mM, and a moderate P concentration, specifically 0.03 mM.

Furthermore, the result of the Pearson correlation coefficient analysis showed that the N concentration in the medium had a strong negative correlation (-0.584) with the accumulation of biomass, which means that the latter will increase as the concentration of N in the medium decreases (Table 2). In addition, the N:P ratio had a moderate negative correlation with biomass accumulation (-0.300), which indicates that the accumulation of biomass increases as the N:P ratio decreases. However, there was no significant correlation between P concentration and biomass accumulation (-0.123).

The optimum N:P ratio for *Spirogyra* sp. biomass accumulation was 38.4. This value aligned with the optimum value of the N:P ratio for macroalgae growth, which was 30 (Lubsch and Timmermans 2018). The results of this study also showed that a high P concentration along with a lower N:P ratio could increase the accumulation of biomass in *Spirogyra* sp. This could be due to the higher P uptake in the medium accompanied by low N:P ratio

TABLE 1 Biomass accumulation in *Spirogyra* sp. on the 14<sup>th</sup> day.

P concentration (mM)	N concentration (mM)			
	1.1	2.2	4.4	6.6
0.01	382 <sup>b</sup>	332 <sup>bc</sup>	296 <sup>c</sup>	259 <sup>d</sup>
0.03	485 <sup>a</sup>	394 <sup>b</sup>	221 <sup>e</sup>	194 <sup>f</sup>
0.06	308 <sup>bc</sup>	260 <sup>d</sup>	188 <sup>f</sup>	258 <sup>d</sup>
0.09	342 <sup>bc</sup>	321 <sup>bc</sup>	262 <sup>d</sup>	310 <sup>bc</sup>

Note: <sup>a,b,c</sup> shows significant difference between treatments ( $p < 0.05$ ).

TABLE 2 Pearson correlation coefficient analysis for the effect of N concentration, P concentration, and N:P ratio on biomass accumulation in *Spirogyra* sp. on the 14<sup>th</sup> day.

Parameter	N	P	N:P Ratio
Pearson Correlation	-0.584*	-0.123	-0.300*
Significance (2-tailed)	>0.001	0.405	0.038

Note: \* shows significant correlation ( $p < 0.05$ ).

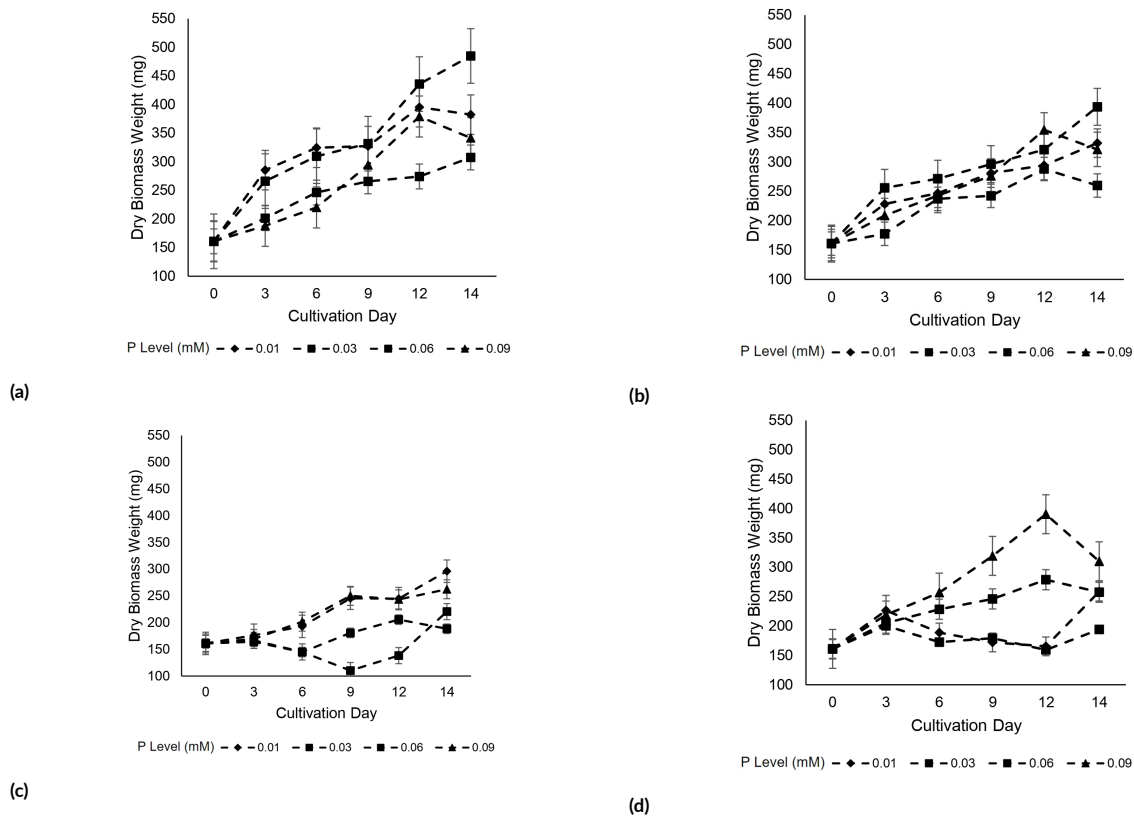


FIGURE 3 Growth curve of *Spirogyra* sp. in medium with N concentration of (a) 1.1, (b) 2.2, (c) 4.4, and (d) 6.6 mM.

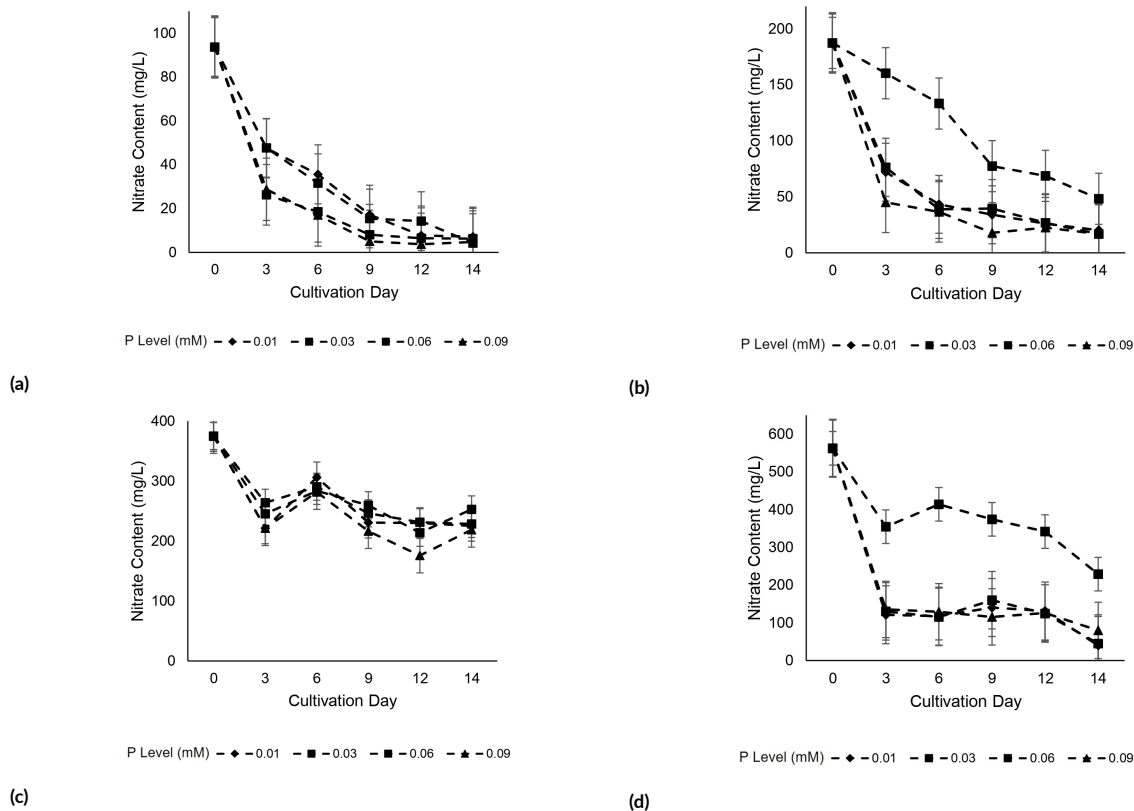


FIGURE 4 Nitrate consumption curve of *Spirogyra* sp. in medium with N concentration of (a) 1.1, (b) 2.2, (c) 4.4, and (d) 6.6 mM.

(Choi and Lee 2015; Figler et al. 2021). High P uptake increases biomass accumulation since algae require P for energy metabolism, protein synthesis, and starch production, as well as the formation of proteins, carbohydrates, cell structures, and cell membrane stabilizers (Xing et al. 2021).

In this study, all treatments showed biomass accumulation on day 3. It occurred because algae require N to form biomass. However, higher N concentrations can also reduce the accumulation of biomass in *Spirogyra* sp., as seen in the cases of the algae cultivated in the N concentrations of 4.4 and 6.6 mM. High concentrations of N may induce an increase in nitrate reductase enzyme activity in cells (Afonso et al. 2022). This enzyme reduces nitrate to nitrite. Nitrite is then reduced to ammonium by the enzyme nitrite reductase, which causes an accumulation of toxic ammonium in cells and therefore reduces the accumulation of biomass (Wang et al. 2019).

A previous study on macroalgae, *Cladophora glomerata*, also showed a decrease in biomass accumulation at high nitrate concentrations, with the highest growth rate at a nitrate concentration of 100 mg/L (Farahdiba et al. 2020). Beyond this concentration, the growth rate of macroalgae tends to decrease. A low concentration of nitrate is also disadvised as it can inhibit the growth of macroalgae. The results of another study showed that the optimum N concentration in the growth medium of macroalgae, *Chaetomorpha aerea*, was 1.5 g/L (Satpati and Pal 2020). N concentrations above 1.5 g/L led to a decrease in biomass accumulation.

TABLE 3 Astaxanthin content in *Spirogyra* sp.

No	N/P Concentration (mM)	Cultivation Time (days)			
		3	6	9	12
1	1.1/0.01	55.3 <sup>bc</sup>	61 <sup>ab</sup>	67.3 <sup>b</sup>	268.7 <sup>a</sup>
2	1.1/0.03	131.7 <sup>ab</sup>	56 <sup>ab</sup>	206.5 <sup>a</sup>	n.d. <sup>b</sup>
3	1.1/0.06	n.d. <sup>c</sup>	n.d. <sup>c</sup>	n.d. <sup>b</sup>	n.d. <sup>b</sup>
4	1.1/0.09	211 <sup>a</sup>	n.d. <sup>c</sup>	n.d. <sup>b</sup>	n.d. <sup>b</sup>
5	2.2/0.01	n.d. <sup>c</sup>	72 <sup>a</sup>	n.d. <sup>b</sup>	n.d. <sup>b</sup>
6	2.2/0.03	n.d. <sup>c</sup>	n.d. <sup>c</sup>	n.d. <sup>b</sup>	n.d. <sup>b</sup>
7	2.2/0.06	4 <sup>c</sup>	n.d. <sup>c</sup>	237 <sup>a</sup>	206 <sup>a</sup>
8	2.2/0.09	20.3 <sup>c</sup>	n.d. <sup>c</sup>	76.3 <sup>b</sup>	n.d. <sup>b</sup>
9	4.4/0.01	n.d. <sup>c</sup>	n.d. <sup>c</sup>	4.2 <sup>b</sup>	n.d. <sup>b</sup>
10	4.4/0.03	n.d. <sup>c</sup>	n.d. <sup>c</sup>	n.d. <sup>b</sup>	n.d. <sup>b</sup>
11	4.4/0.06	n.d. <sup>c</sup>	n.d. <sup>c</sup>	n.d. <sup>b</sup>	n.d. <sup>b</sup>
12	4.4/0.09	n.d. <sup>c</sup>	n.d. <sup>c</sup>	n.d. <sup>b</sup>	n.d. <sup>b</sup>
13	6.6/0.01	6.3 <sup>c</sup>	n.d. <sup>c</sup>	16 <sup>b</sup>	24.5 <sup>b</sup>
14	6.6/0.03	n.d. <sup>c</sup>	n.d. <sup>c</sup>	211 <sup>a</sup>	n.d. <sup>b</sup>
15	6.6/0.06	n.d. <sup>c</sup>	15.5 <sup>c</sup>	n.d. <sup>b</sup>	n.d. <sup>b</sup>
16	6.6/0.09	54.5 <sup>bc</sup>	34 <sup>bc</sup>	n.d. <sup>b</sup>	16.7 <sup>b</sup>

Note: <sup>a,b,c</sup> shows significant difference between treatments ( $p < 0.05$ ). n.d. = not detected.

### 3.2. Effect of N concentration, P concentration, and N:P ratio on *Spirogyra* sp. nitrate consumption

There was a significant decrease in nitrate concentration in the medium on the 3<sup>rd</sup> day of cultivation (Figure 4). This may have reflected the ability of macroalgae to absorb nitrate effectively and efficiently from the first day of cultivation due to its large surface-area-per-volume ratio (Wang et al. 2014; Farahdiba et al. 2020). Macroalgae can also absorb large amounts of nitrate as it can utilize all of the nitrate present in the medium when administered in excess (Sánchez De Pedro et al. 2013).

Nitrate concentrations in the medium tended to fluctuate after the 6<sup>th</sup> day of cultivation. This may be due to the reduced absorption rate and the release of organic nitrogen by macroalgae into the environment (Hardison et al. 2013). In this study, a trend was identified whereby nitrate uptake increased with a decreasing P concentration in the medium. However, the difference was not particularly significant. Previous studies have reported the same phenomenon, citing nitrate removals in media with N:P ratios of 1–10, 11–20, and 21–30 of 78.35 ± 8.23%, 83.90 ± 2.90%, and 82.81 ± 2.81% respectively (Choi and Lee 2015). In another study, the nitrate removal in media with N:P ratios of 1.7 and 5.8 was 100 % (Figler et al. 2021).

### 3.3. Effect of N concentration, P concentration, and N:P ratio on *Spirogyra* sp. astaxanthin accumulation

The results of the *Spirogyra* sp. extract analysis using HPLC showed a significant difference in astaxanthin content between treatments (Table 3). The highest astaxanthin content was found on day 12 in the macroalgae that were cultivated in the medium with the lowest N/P concentration (1.1/0.01 mM).

Astaxanthin was found to accumulate in *Spirogyra* sp. at lower and higher concentrations of N, namely 1.1; 2.2; and 6.6 mM. It may be caused by both a deficiency and excess of N in the medium. In higher plants and green algae, such as *C. zofingiensis*, environmental stress such as nitrogen starvation can increase ROS which are derivatives of NADPH oxidase (Sun and Zhang 2021). This increase in ROS can induce the accumulation of astaxanthin in cells. A high N concentration in the medium may produce an increase in ammonia concentration that is toxic to *Spirogyra* sp. (Wang et al. 2019). Excessive amounts of ammonia lead to ROS formation which induces astaxanthin production (Shen et al. 2020).

The Pearson correlation coefficient showed that the P concentration and N:P ratio did not have a significant correlation with the accumulation of astaxanthin. However, N concentration was shown to correlate with astaxanthin accumulation on day 3 (Table 4).

The correlation test results showed that on the 3<sup>rd</sup> day, the N concentration had a moderate negative correlation with the accumulation of astaxanthin, where the accumulation would increase with the reduced availability of nitrate in the medium. The same phenomenon was found in a pre-

**TABLE 4** Effect of N concentration, P concentration, and N:P ratio on astaxanthin accumulation in *Spirogyra* sp.

Cultivation Day	Parameter	N	P	N:P Ratio
3	Pearson Correlation	-0.350*	0.159	-0.269
	Significance (2-tailed)	0.018	0.298	0.074
6	Pearson Correlation	-0.293	-0.269	-0.156
	Significance (2-tailed)	0.063	0.089	0.331
9	Pearson Correlation	-0.136	-0.083	-0.780
	Significance (2-tailed)	0.398	0.605	0.626
12	Pearson Correlation	-0.229	-0.169	-0.094
	Significance (2-tailed)	0.130	0.266	0.538

Note: \* shows significant correlation ( $p < 0.05$ )

vious study where nitrate starvation on *H. pluvialis* cultivation increased the astaxanthin content in cells from 500 pg/cell (control) to 1500 pg/cell (nitrate starvation) (Scibilia et al. 2015). In another study, the astaxanthin content at  $\text{NaNO}_3$  concentrations of 0.25 and 0.75 g/L was 0.2% of the fresh weight of *H. pluvialis* biomass, while the astaxanthin contents at lower concentrations of 0.125 g/L and 0 g/L respectively were 0.26% and 0.3% wet weight (Ding et al. 2019).

When algae undergo nitrogen starvation, it induces chlorophyll and protein biosynthesis impairment, redirecting the metabolism to lipids and carotenoid accumulation

(Scibilia et al. 2015). Nitrogen deficiency-induced abiotic stress can also increase the activity of NADPH oxidase, which produces a large amount of ROS quickly (Sun and Zhang 2021). The high ROS cellular content then stimulates astaxanthin production as a defensive mechanism. In a previous study on *Haematococcus pluvialis*, nitrogen stress led to up-regulation of the IPPI and HDR genes in the MEP pathway that supplies IPP (isopentanyl diphosphate) which is a precursor for astaxanthin biosynthesis (Zhao et al. 2020).

In contrast, P concentration and N:P ratio do not significantly relate to the astaxanthin content in *Spirogyra* sp.

**TABLE 5** Astaxanthin productivity in *Spirogyra* sp.

No	N/P Concentration (mM)	Cultivation Time (d)	Dry Biomass Weight (mg)	Astaxanthin Content ( $\mu\text{g}/\text{mg}$ )	Productivity ( $\mu\text{g}/\text{cm}^2/\text{d}$ )
1	1.1/0.01	3	285	0.055	0.027
		6	324	0.061	0.017
		9	327	0.067	0.013
		12	395	0.269	0.046
2	1.1/0.03	3	266	0.132	0.060
		6	310	0.056	0.015
		9	332	0.207	0.039
3	1.1/0.06	3	202	0	0.000
4	1.1/0.09	3	188	0.211	0.068
5	2.2/0.01	3	229	0	0.000
		6	247	0.072	0.015
6	2.2/0.03	3	256	0	0.000
7	2.2/0.06	3	178	0.004	0.001
		6	237	0	0.000
		9	242	0.237	0.033
		12	288	0.206	0.026
8	2.2/0.09	3	209	0.020	0.007
		6	243	0	0.000
		9	276	0.076	0.012
		12	355	0	0.000
9	4.4/0.01	3	176	0	0.000
		6	193	0	0.000
		9	245	0.004	0.001
		12	245	0	0.000

TABLE 5 (continued).

No	N/P Concentration (mM)	Cultivation Time (d)	Dry Biomass Weight (mg)	Astaxanthin Content ( $\mu\text{g}/\text{mg}$ )	Productivity ( $\mu\text{g}/\text{cm}^2/\text{d}$ )
10	4.4/0.03	3	167	0	0.000
11	4.4/0.06	3	164	0	0.000
12	4.4/0.09	3	169	0	0.000
13	6.6/0.01	3	227	0.006	0.002
		6	189	0	0.000
		9	172	0.016	0.002
		12	165	0.025	0.002
14	6.6/0.03	3	200	0	0.000
		6	172	0	0.000
		9	179	0.211	0.022
		12	159	0	0.000
15	6.6/0.06	3	205	0	0.000
		6	229	0.016	0.003
		9	246	0	0.000
		12	279	0	0.000
16	6.6/0.09	3	219	0.054	0.021
		6	257	0.034	0.008
		9	319	0	0.000
		12	390	0.017	0.003

However, an eminently high N:P ratio (excessive nitrogen or insufficient phosphorus) or an eminently low N:P ratio (very low quantity of nitrogen or excessive phosphorus) is not favorable for astaxanthin production as it may not support the sustainability of the algae nor be able to induce astaxanthin production in *Spirogyra* sp. As a rule of thumb, a lower nitrogen content is more favorable as it leads to higher astaxanthin production. In addition, the medium must contain sufficient phosphorous for the algae to provide optimum growth conditions and sustain the viability of the algae (Ali et al. 2022). In this study, fluctuations were observed in the astaxanthin content of the *Spirogyra* sp. biomass. These may have occurred as *Spirogyra* sp. responds to its environmental conditions, which in this case consisted of an abundance or insufficiency of nutrients in the cultivation medium. A low N and P concentration in the medium would affect ROS formation, therefore increasing the production of astaxanthin in the cells. Alternatively, the astaxanthin contents within the biomass may have fallen due to reacting with the ROS inside the cells, to form astaxanthin epoxide, astaxanthin endoperoxide, or apo-astaxanthin (Nishino et al. 2016).

### 3.4. *Spirogyra* sp. astaxanthin productivity estimation

Productivity was estimated to determine the best cultivation conditions and duration. This condition was necessary because the increase in astaxanthin was associated with the increase in biomass. Astaxanthin productivity was calculated by considering the astaxanthin content in the biomass, the dry weight of the biomass, the surface area of the cultivation container, and the cultivation time. The highest biomass accumulation was found in biomass

that was cultivated in a medium with a low N concentration (Table 5). These conditions are therefore the best in which to obtain large amounts of biomass. Furthermore, the highest accumulation of astaxanthin was found in the variation of N/P 1.1/0.09 mM on the 3<sup>rd</sup> day of cultivation. The combination of high biomass and astaxanthin accumulation and low cultivation time in this treatment resulted in higher astaxanthin productivity.

### 3.5. Kinetic modeling of *Spirogyra* sp. growth and astaxanthin production

The Haldane equation was used to model biomass growth and nitrate consumption as it considers the biomass accumulation from nutrients and nutrient consumption to deliver better modeling results. Based on the parameter estimation results using research data and the Haldane equation, the average maximum growth rate was  $0.17 \pm 0.04 \text{ d}^{-1}$  (Table 6). This value previously reported *Spirogyra* sp. Growth rates, i.e.  $0.07 \text{ d}^{-1}$  in BG medium (Yu et al. 2022) and  $0.04 \text{ d}^{-1}$  in brackish water (Sadiq et al. 2018). It was also higher than the growth rate of the macroalgae *Chladophora glomerata*, which was  $0.08 \text{ d}^{-1}$  (Farahdiba et al. 2020), but lower than that of *H. pluvialis* under nitrogen starvation conditions, at  $0.26 \pm 0.03 \text{ d}^{-1}$  (Vega-Ramon et al. 2021).

The  $k_N$  parameter which was  $72.8 \pm 25.0 \text{ mg/L}$  indicated that *Spirogyra* sp. requires the availability of sufficient nitrate to grow rapidly. The  $k_i$  parameter, at  $292.44 \pm 99.9 \text{ mg/L}$ , indicated that this level of nitrate concentration could inhibit the growth of *Spirogyra* sp. up to half the maximum. The yield of biomass per nitrate ( $Y_N$ ) appeared to decrease as the initial nitrate concentration in-

**TABLE 6** Parameter of *Spirogyra* sp. growth model using Haldane equation.

No	N/P Concentration (mM)	$\mu_{\max}$ (d <sup>-1</sup> )	$k_N$ (mg/L)	$Y_{\text{biomass/nitrate}}$ (g/g)	$k_i$ (mg/L)
1	1.1/0.01	0.19	50	2.31	200
2	1.1/0.03	0.19	50	1.43	300
3	1.1/0.06	0.20	100	1.35	400
4	1.1/0.09	0.20	50	1.48	360
5	2.2/0.01	0.20	100	0.69	360
6	2.2/0.03	0.20	64	0.85	360
7	2.2/0.06	0.10	100	0.87	283
8	2.2/0.09	0.20	50	0.62	360
9	4.4/0.01	0.20	50	0.34	360
10	4.4/0.03	0.10	100	0.38	100
11	4.4/0.06	0.10	100	0.36	100
12	4.4/0.09	0.20	50	0.34	360
13	6.6/0.01	0.14	100	0.34	256
14	6.6/0.03	0.15	100	0.34	161
15	6.6/0.06	0.20	50	0.34	360
16	6.6/0.09	0.20	50	0.34	360

creased. This could be due to the assimilation of nitrate by *Spirogyra* sp. that was not used as a building block for biomass.

Astaxanthin production was then modeled using the Luedeking–Piret equation to determine whether astaxanthin is a growth-associated product, non-growth-associated product, or partially associated in *Spirogyra* sp. Parameter estimation was conducted to obtain the modeling parameters (Table 7).

The parameter estimation results did not show a trend. This means that astaxanthin could be produced during growth or after it has reached its stationary phase. The

**TABLE 7** Luedeking–Piret parameters for astaxanthin production model in *Spirogyra* sp.

No	N/P Concentration (mM)	$\alpha$	$\beta$	$k_A$
1	1.1/0.01	-0.13	0.03	0.01
2	1.1/0.03	0.76	-0.05	0.04
3	1.1/0.06	0	0	0
4	1.1/0.09	0.55	-0.03	0.05
5	2.2/0.01	0.27	-0.01	0.07
6	2.2/0.03	0	0	0
7	2.2/0.06	0.44	-0.07	0.03
8	2.2/0.09	0.20	-0.01	0.04
9	4.4/0.01	0.08	0.01	0.03
10	4.4/0.03	0	0	0
11	4.4/0.06	0	0	0
12	4.4/0.09	0	0	0
13	6.6/0.01	-0.41	0.01	0.01
14	6.6/0.03	1.98	-0.02	0.08
15	6.6/0.06	0.07	0.00	0.02
16	6.6/0.09	0.05	0.00	0.03

astaxanthin content in the biomass increased in both N/P treatments of 1.1/0.01 and 6.6/0.01 mM. Meanwhile, in other treatments, the astaxanthin content decreased. This results in a negative  $\beta$  value because metabolite production ceases when the amount of biomass tends to be constant. In the N/P treatments 1.1/0.01 and 6.6/0.01 mM, the increase in astaxanthin content in the biomass was related to the amount of biomass however it was not related to the growth rate. This may have been caused by a continued increase in the astaxanthin content even as the growth rate began to fall.

The kinetic model developed using the Haldane equation succeeded in modeling the growth of *Spirogyra* sp. at an intermediate N concentration, of 2.2 mM (Figure 5). The  $R^2$  value was 0.821 for biomass growth and 0.930 for nitrate consumption.

At higher N concentrations, e.g. 6.6 mM, the Haldane equation produced a good growth model ( $R^2 = 0.884$ ) but was unable to give a representative nitrate consumption model ( $R^2 = 0.664$ ). This may have been due to the surge in nitrate uptake from day 0 to day 3 which the Haldane equation was unable to model (Figure 6).

Overall, the Haldane model properly models the growth of *Spirogyra* sp. and its nitrate consumption. It also models growth kinetics better than the Monod equation because it considers the occurrence of growth inhibition by high nitrate concentrations. In previous research, the Haldane equation was also found to be more representative than the model formed by the Monod and Steele equations to represent the effect of light inhibition (Krichen et al. 2021). However, other variables such as biomass mortality as a function of nitrate and surge uptake activity are not included in the Haldane model and should be considered to obtain a more representative model.

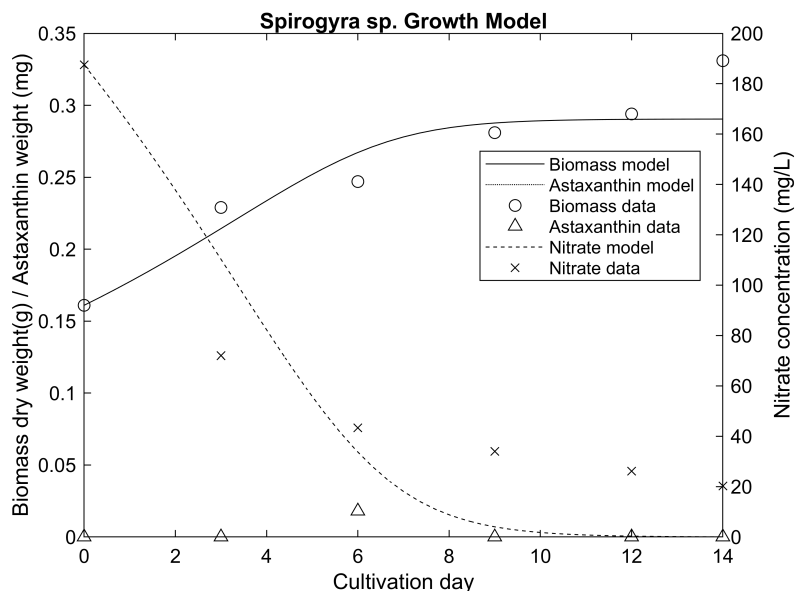


FIGURE 5 Kinetic modeling of *Spirogyra* sp. growth in BG medium with N/P concentration 2.2/0.01 mM.

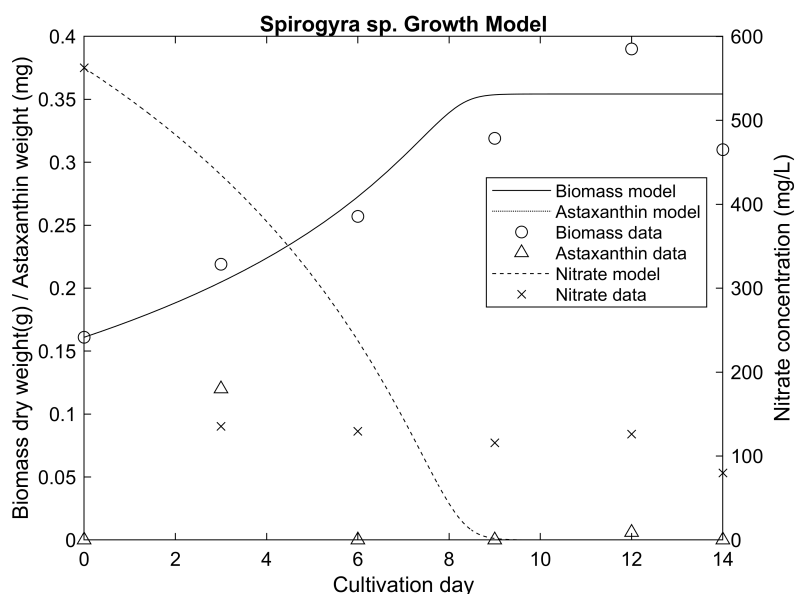


FIGURE 6 Kinetic modeling of *Spirogyra* sp. growth in BG medium with N/P concentration 6.6/0.09 mM.

### 4. Conclusions

This study demonstrates that N concentration and the N:P ratio affect *Spirogyra* sp. biomass accumulation. The accumulation of biomass increases with the addition of N up to 1.1 mM and an N:P ratio up to 13:1. Meanwhile, the addition of P in the concentration of 0.01–0.09 mM shows no effect on biomass accumulation. The accumulation of astaxanthin in *Spirogyra* sp. increases at low concentrations of N (up to 1.1 mM), while P concentration and N:P ratio show no significant effect on astaxanthin accumulation. Kinetic modeling using the Haldane equation yields a representative growth and nitrate consumption model. Based

on Luedeking–Piret modeling, the accumulation of astaxanthin in *Spirogyra* sp. is partially associated with growth.

### Acknowledgments

This work was financially supported by Research, Community Services, and Innovation Program of Institut Teknologi Bandung, Indonesia grant number 1110/11.C02.2/KU/2020.

## Authors' contributions

NDZ, MYCP, and IPIS designed the research. EM and KHB verified the methods for the experiment. NDZ, MYCP, and IPIS conducted the experiment and collected the data. NDZ analyzed the data and conducted the simulation. EM and KHB supervised the process. NDZ and IPIS wrote the manuscript in consultation with EM.

## Competing interests

The authors declare that the research was conducted in the absence of any commercial or financial relationships that could be construed as a potential conflict of interest.

## References

- Abdulrasheed M, Zulkharnain A, Zakaria NN, Ahmad Roslee AF, Khalil KA, Napis S, Convey P, Gomez-Fuentes C, Ahmad SA. 2020. Response surface methodology optimization and kinetics of diesel degradation by a cold-adapted antarctic bacterium, *Arthrobacter* sp. strain AQ5-05. *Sustain.* 12(17):6966. doi:10.3390/SU12176966.
- Afonso C, Bragança AR, Rebelo BA, Serra TS, Abranches R. 2022. Optimal nitrate supplementation in *Phaeodactylum tricornutum* culture medium increases biomass and fucoxanthin production. *Foods* 11(4):568. doi:10.3390/foods11040568.
- Ali HEA, Vorisek F, Dowd SE, Kesner S, Song Y, Qian D, Crocker M. 2022. Formation of Lutein,  $\beta$ -carotene and astaxanthin in a *Coelastrella* sp. isolate. *Molecules* 27(20):6950. doi:10.3390/molecules27206950.
- Allen MM, Stanier RY. 1968. Selective isolation of blue-green algae from water and soil. *J. Gen. Microbiol.* 51(2):203–209. doi:10.1099/00221287-51-2-203.
- Ambati RR, Moi PS, Ravi S, Aswathanarayana RG. 2014. Astaxanthin: Sources, extraction, stability, biological activities and its commercial applications - A review. *Mar Drugs* 12(1):128–152. doi:10.3390/md12010128.
- Choi HJ, Lee SM. 2015. Effect of the N/P ratio on biomass productivity and nutrient removal from municipal wastewater. *Bioprocess Biosyst. Eng.* 38(4):761–766. doi:10.1007/s00449-014-1317-z.
- Cong XY, Miao JK, Zhang HZ, Sun WH, Xing LH, Sun LR, Zu L, Gao Y, Leng KL. 2019. Effects of drying methods on the content, structural isomers, and composition of astaxanthin in Antarctic krill. *ACS Omega* 4(19):17972–17980. doi:10.1021/acsomega.9b01294.
- Ding D, Chen S, Peng S, Jiang C, Zheng L, Li J. 2019. Strategies of phosphorus utilization in an astaxanthin-producing green alga *Haematococcus pluvialis*, a comparison with a bloom-forming cyanobacterium *Microcystis wesenbergii*. *Aquat. Ecol.* 53(4):679–688. doi:10.1007/s10452-019-09718-z.
- Ekpe L, Inaku K, Ekpe V. 2018. Antioxidant effects of astaxanthin in various diseases a review. *J. Mol. Pathophysiol.* 7(1):1–6. doi:10.5455/jmp.20180627120817.
- Ermavitalini D, Rukhmana SY, Meidina T, Baskoro LPDC, Saputro TB, Ni'matuzahroh, Purnobasuki H. 2021. Astaxanthin-producing microalgae identification using 18S rRNA: Isolates from Bangkalan Mangrove Waters and Sowan Tuban Northern Waters, East Java, Indonesia. *J. Trop. Biodivers. Biotechnol.* 6(3):64882. doi:10.22146/JTBB.64882.
- Fan F, Wan M, Huang J, Wang W, Bai W, He M, Li Y. 2021. Modeling of astaxanthin production in the two-stage cultivation of *Haematococcus pluvialis* and its application on the optimization of vertical multi-column airlift photobioreactor. *Algal Res.* 58:102301. doi:10.1016/j.algal.2021.102301.
- Farahdiba AU, Hidayah EN, Asmar GA, Myint YW. 2020. Growth and removal of nitrogen and phosphorus by a macroalgae *Cladophora glomerata* under different nitrate concentrations. *Nat. Environ. Pollut. Technol.* 19(2):809–813. doi:10.46488/NEPT.2020.V19I02.038.
- Figler A, Márton K, B-Béres V, Bácsi I. 2021. Effects of nutrient content and nitrogen to phosphorous ratio on the growth, nutrient removal and desalination properties of the green alga *Coelastrum morus* on a laboratory scale. *Energies* 14(8):2112. doi:10.3390/en14082112.
- Grand Review Research. 2022. San Fransisco: Grand View Research. <https://www.grandviewresearch.com/industry-analysis/global-astaxanthin-market>. Modified 2022 Dec 27; Accessed 2023 Feb 10.
- Hardison AK, Canuel EA, Anderson IC, Tobias CR, Veuger B, Waters MN. 2013. Microphytobenthos and benthic macroalgae determine sediment organic matter composition in shallow photic sediments. *Biogeosciences* 10(8):5571–5588. doi:10.5194/bg-10-5571-2013.
- Karnila R, Hasan B, Ilza M, Leksono T, Ahmad MA. 2021. Astaxanthin extraction of vanname shrimp (*Litopenaeus vanname*) using palm oil. *IOP Conf. Ser. Earth Environ. Sci.* 695(1):012056. doi:10.1088/1755-1315/695/1/012056.
- Kohandel Z, Farkhondeh T, Aschner M, Samarghandian S. 2021. Nrf2 a molecular therapeutic target for astaxanthin. *Biomed. Pharmacother.* 137:111374. doi:10.1016/j.biopha.2021.111374.
- Krichen E, Rapaport A, Le Floc'h E, Fouilland E. 2021. A new kinetics model to predict the growth of micro-algae subjected to fluctuating availability of light. *Algal Res.* 58:102362. doi:10.1016/j.algal.2021.102362.
- Kurniawati P, Gusrianti R, Dwisiwi BB, Purbaningtias TE, Wiyantoko B. 2017. Verification of spectrophotometric method for nitrate analysis in water samples. *AIP*

- Conf. Proc. 1911:020012. doi:10.1063/1.5016005.
- Li F, Cai M, Wu Y, Lian Q, Qian Z, Luo J, Zhang Y, Zhang N, Li C, Huang X. 2022. Effects of nitrogen and light intensity on the astaxanthin accumulation in motile cells of *Haematococcus pluvialis*. *Front. Mar. Sci.* 9:909237. doi:10.3389/fmars.2022.909237.
- Lima SGM, Freire MCLC, Oliveira VdS, Solisio C, Converti A, de Lima ÁAN. 2021. Astaxanthin delivery systems for skin application: A review. *Mar. Drugs* 19(9):511. doi:10.3390/MD19090511.
- Liu Y. 2018. Optimization study Of biomass And astaxanthin production by *Haematococcus pluvialis* under minkery wastewater cultures. Thesis, Dalhousie University, Halifax.
- Lubsch A, Timmermans K. 2018. Uptake kinetics and storage capacity of dissolved inorganic phosphorus and corresponding N:P dynamics in *Ulva lactuca* (Chlorophyta). *J. Phycol.* 54(2):215–223. doi:10.1111/jpy.12612.
- Munir N, Imtiaz A, Sharif N, Naz S. 2015. Optimization of growth conditions of different algal strains and determination of their lipid contents. *J. Anim. Plant Sci.* 25(2):546–553.
- Nalcaci OO, Böke N, Ovez B. 2011. Potential of the bacterial strain *Acidovorax avenae* subsp. *avenae* LMG 17238 and macro algae *Gracilaria verrucosa* for denitrification. *Desalination* 274(1-3):44–53. doi:10.1016/j.desal.2011.01.067.
- Nishino A, Maoka T, Yasui H. 2016. Analysis of reaction products of astaxanthin and its acetate with reactive oxygen species using LC/PDA ESI-MS and ESR spectrometry. *Tetrahedron Lett.* 57(18):1967–1970. doi:10.1016/j.tetlet.2016.03.078.
- Pacheco R, Ferreira AF, Pinto T, Nobre BP, Loureiro D, Moura P, Gouveia L, Silva CM. 2015. The production of pigments & hydrogen through a *Spirogyra* sp. biorefinery. *Energy Convers. Manag.* 89:789–797. doi:10.1016/j.enconman.2014.10.040.
- Régnier P, Bastias J, Rodriguez-Ruiz V, Caballero-Casero N, Caballo C, Sicilia D, Fuentes A, Maire M, Crepin M, Letourneur D, Gueguen V, Rubio S, Pavon-Djavid G. 2015. Astaxanthin from *Haematococcus pluvialis* prevents oxidative stress on human endothelial cells without toxicity. *Mar. Drugs* 13(5):2857–2874. doi:10.3390/md13052857.
- Ruen-ngam D, Shotipruk A, Pavasant P. 2010. Comparison of extraction methods for recovery of astaxanthin from *Haematococcus pluvialis*. *Sep. Sci. Technol.* 46(1):64–70. doi:10.1080/01496395.2010.493546.
- Sadiq UAFM, Yow ME, Jamaian SS. 2018. The extended Monod model for microalgae growth and nutrient uptake in different wastewaters. *Int. J. Eng. Technol.* 7(4.30):200. doi:10.14419/ijet.v7i4.30.22120.
- Sánchez De Pedro R, Niell FX, Carmona R. 2013. Differential nutrient uptake by two segregated red algae in an estuarine intertidal zone. *Phycologia* 52(6):461–471. doi:10.2216/13-147.1.
- Satpati GG, Pal R. 2020. Effects of nitrogen, phosphorus, EDTA and sodium chloride on biomass and lipid accumulation of *Chaetomorpha aerea*. *Curr. Bot.* 11:152–158. doi:10.25081/cb.2020.v11.6223.
- Scibilia L, Girolomoni L, Berteotti S, Alboresi A, Ballottari M. 2015. Photosynthetic response to nitrogen starvation and high light in *Haematococcus pluvialis*. *Algal Res.* 12:170–181. doi:10.1016/j.algal.2015.08.024.
- Serri NA, Anbalagan L, Norafand NZ, Kassim MA, Abu Mansor MS. 2020. Preliminary study on the growth of *Tetraselmis suecica* in centred-light photobioreactor (CLPBR). *IOP Conf. Ser. Mater. Sci. Eng.* 716(1):012008. doi:10.1088/1757-899X/716/1/012008.
- Shen Y, Qiu S, Chen Z, Zhang Y, Trent J, Ge S. 2020. Free ammonia is the primary stress factor rather than total ammonium to *Chlorella sorokiniana* in simulated sludge fermentation liquor. *Chem. Eng. J.* 397:125490. doi:10.1016/j.cej.2020.125490.
- Simanjuntak D. 2021. Modeling of growth kinetics and lipid production in *Spirogyra* sp. cultures experiencing nitrogen deficiency. Bachelor thesis, Institut Teknologi Bandung, Bandung.
- Stachowiak B, Szulc P. 2021. Astaxanthin for the food industry. *Molecules* 26(9):2666. doi:10.3390/molecules26092666.
- Sun D, Zhang Z. 2021. Reactive oxygen species derived from NADPH oxidase regulate astaxanthin and total fatty acid accumulation in *Chromochloris zofingiensis*. *J. Appl. Phycol.* 33(2):819–827. doi:10.1007/s10811-020-02327-6.
- Takano T, Higuchi S, Ikegaya H, Matsuzaki R, Kawachi M, Takahashi F, Nozaki H. 2019. Identification of 13 *Spirogyra* species (Zygnemataceae) by traits of sexual reproduction induced under laboratory culture conditions. *Sci. Rep.* 9(1):7458. doi:10.1038/s41598-019-43454-6.
- Tharek A, Jamaluddin H, Salleh MMD, Yahya NA, Kaha M, Hara H, Iwamoto K, Mohamad SE. 2020. Astaxanthin production by tropical microalgae strains isolated from environment in Malaysia. *Asian J. Microbiol., Biotechnol. Environ. Sci.* 22(1):168–173.
- Tran TN, Tran QV, Huynh HT, Hoang NS, Nguyen HC, Ngo DN. 2019. Astaxanthin production by newly isolated *Rhodospiridium toruloides*: Optimization of medium compositions by response surface methodology. *Not. Bot. Horti Agrobot. Cluj-Napoca* 47(2):320–327. doi:10.15835/nbha47111361.
- Vega-Ramon F, Zhu X, Savage TR, Petsagkourakis P, Jing K, Zhang D. 2021. Kinetic and hybrid modeling for yeast astaxanthin production under uncertainty. *Biotechnol. Bioeng.* 118(12):4854–4866. doi:10.1002/bit.27950.
- Wang C, Lei A, Zhou K, Hu Z, Hao W, Yang J. 2014. Growth and nitrogen uptake characteristics reveal outbreak mechanism of the opportunistic macroalga *Gracilaria tenuistipitata*. *PLoS One* 9(10):e108980. doi:10.1371/journal.pone.0108980.

- Wang J, Zhou W, Chen H, Zhan J, He C, Wang Q. 2019. Ammonium nitrogen tolerant *Chlorella* strain screening and its damaging effects on photosynthesis. *Front. Microbiol.* 10:3250. doi:10.3389/fmicb.2018.03250.
- Wongsawad P, Peerapornpisal Y. 2015. Morphological and molecular profiling of *Spirogyra* from North-eastern and Northern Thailand using inter simple sequence repeat (ISSR) markers. *Saudi J. Biol. Sci.* 22(4):382–389. doi:10.1016/j.sjbs.2014.10.004.
- Xing Y, Guo L, Wang Y, Zhao Y, Jin C, Gao M, Ji J, She Z. 2021. An insight into the phosphorus distribution in extracellular and intracellular cell of *Chlorella vulgaris* under mixotrophic cultivation. *Algal Res.* 60:102482. doi:10.1016/j.algal.2021.102482.
- Yu H, Kim J, Rhee C, Shin J, Shin SG, Lee C. 2022. Effects of different pH control strategies on microalgae cultivation and nutrient removal from anaerobic digestion effluent. *Microorganisms* 10(2):357. doi:10.3390/microorganisms10020357.
- Zhang WW, Zhou XF, Zhang YL, Cheng PF, Ma R, Cheng WL, Chu HQ. 2018. Enhancing astaxanthin accumulation in *Haematococcus pluvialis* by coupled light intensity and nitrogen starvation in column photobioreactors. *J. Microbiol. Biotechnol.* 28(12):2019–2028. doi:10.4014/jmb.1807.07008.
- Zhao X, Zhang X, Fu L, Zhu H, Zhang B. 2016. Effect of extraction and drying methods on antioxidant activity of astaxanthin from *Haematococcus pluvialis*. *Food Bioprod. Process.* 99:197–203. doi:10.1016/j.fbp.2016.05.007.
- Zhao Y, Hou Y, Chai W, Liu Z, Wang X, He CQ, Hu Z, Chen S, Wang W, Chen F. 2020. Transcriptome analysis of *Haematococcus pluvialis* of multiple defensive systems against nitrogen starvation. *Enzyme Microb. Technol.* 134:109487. doi:10.1016/j.enzmictec.2019.109487.
- Zhuang Y, Zhu MJ. 2021. Recent developments in astaxanthin production from *Phaffia rhodozyma* and its applications. *Glob. Perspect. Astaxanthin From Ind. Prod. to Food, Heal. Pharm. Appl.* p. 225–251. doi:10.1016/B978-0-12-823304-7.00006-4.